

1 **Supplement**

2 **Effect of stress history on sediment transport and channel adjustment**  
3 **in graded gravel-bed rivers**

4 Chenge An<sup>1,2</sup>, Marwan A. Hassan<sup>2</sup>, Carles Ferrer-Boix<sup>3</sup>, Xudong Fu<sup>1</sup>

5 <sup>1</sup> Department of Hydraulic Engineering, State Key Laboratory of Hydrosience and Engineering, Tsinghua University, Beijing,  
6 China.

7 <sup>2</sup> Department of Geography, The University of British Columbia, Vancouver, BC, Canada.

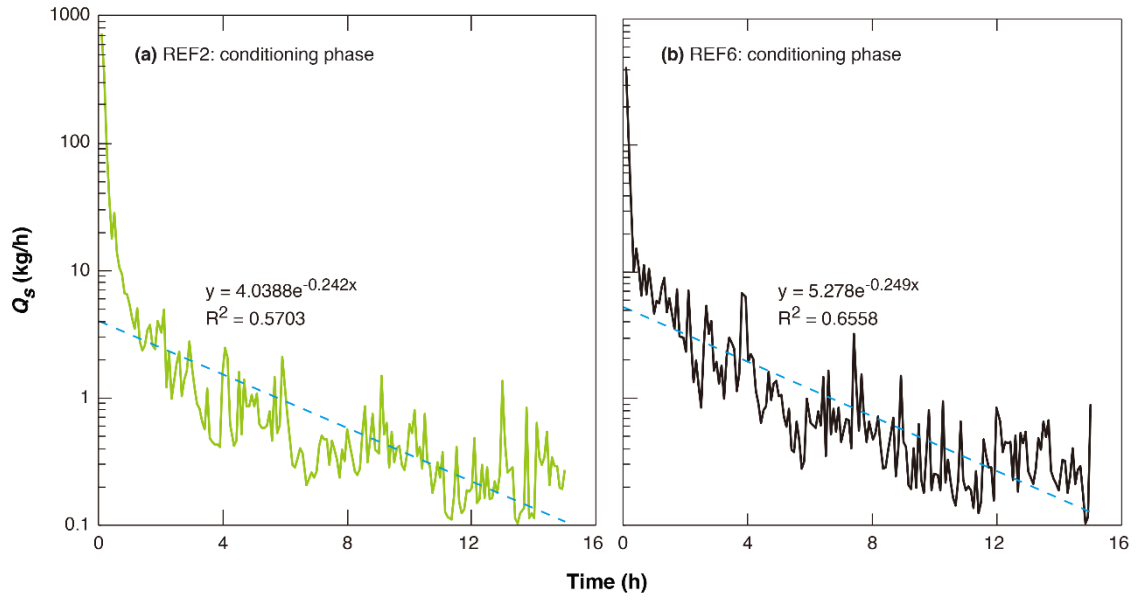
8 <sup>3</sup> Department of Civil and Environmental Engineering, Technical University of Catalonia, Barcelona, Spain.

9 *Correspondence to:* Xudong Fu ([xdfu@tsinghua.edu.cn](mailto:xdfu@tsinghua.edu.cn))

10

11 **S1. Regression of sediment transport rates against the exponential function**

12 In this section, we fit the instantaneous sediment transport rates during the conditioning phase of our experiment by  
13 a two-parameter exponential function. Previous researchers (Haynes and Pender, 2007; Masteller and Finnegan, 2017) have  
14 suggested that the exponential function can be implemented to describe the temporal decrease of sediment transport rate under  
15 conditioning flow. Here two of our experiments with the longest duration of conditioning phase (REF2 (15) and REF6 (15))  
16 are analyzed. Results are shown in Fig. S1. As we can see from the figure, the fitted exponential function can describe the  
17 general decreasing trend of sediment transport rate during the conditioning phase, except at the beginning of the conditioning  
18 phase where the decrease of sediment transport rate is much more significant than predicted by the exponential function.  
19 Moreover, for the two experiments, the exponential function shows very similar values of regression parameters.

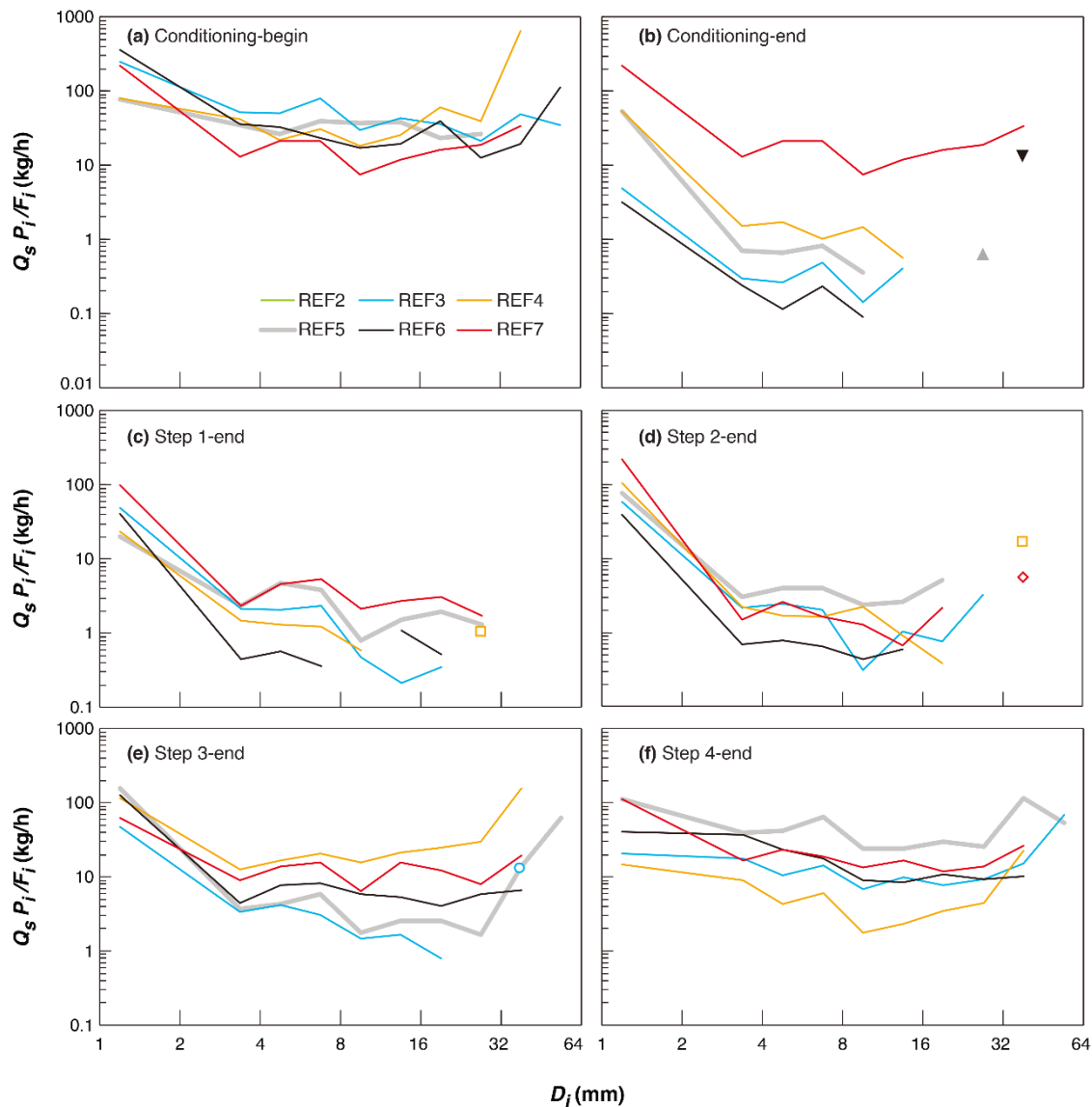


20  
 21 **Figure S1.** Regression of sediment transport rates during the conditioning phase, using an exponential function. (a) REF2 (15);  
 22 (b) REF6 (15). Solid lines denote instantaneous sediment transport rates measured by light table. Dash lines denote calibrated  
 23 exponential functions. The regression parameters and correlation coefficient are also shown in the figure.

## 24 S2. Sediment mobility of each size range during the experiment

25 In this section, we analyze the sediment mobility of each size range during the experiments. Figure S2 shows the  
 26 scaled fractional sediment transport rate  $Q_s p_i / F_i$  at different time of the experiment based on the light table data, where  $p_i$   
 27 denotes the volume fraction of the  $i$ -th size range in the bedload and  $F_i$  denotes the volume fraction of the  $i$ -th size range on  
 28 the bed surface. By scaling on the bed surface fraction, the scaled fractional sediment transport rate thus represents the mobility  
 29 of each size range: the larger the scaled fractional sediment transport rate is, the larger is the sediment mobility of this size  
 30 range. In Fig. S2(a), the sediment mobility of different experiment is similar and each experiment shows an approximately  
 31 horizontal line with the grain size, indicating that equal mobility dominates at the beginning of the conditioning phase. At the  
 32 end of the conditioning phase (as shown in Fig. S2(b)), the mobility among experiments becomes different: the shorter the  
 33 duration of the conditioning phase, the larger is the overall mobility. Moreover, the experiment with the shortest conditioning  
 34 duration (i.e., REF7 (0.25)) is still near equal mobility, except that the mobility of the finest size range is larger than other size  
 35 ranges. Whereas other experiments have become partial mobility with evident selective transport for sediment finer than 16  
 36 mm and almost no mobility for sediment coarser than 16 mm. This agrees with the observation by Ockelford et al. (2019) that  
 37 bedload transport is characterized by equal mobility with no conditioning flow, but becomes more strongly size selective in  
 38 the coarse and fine end members of the distribution as the duration of conditioning flow increases. Two isolated dots are  
 39 observed at the very coarse end in REF5 (5) and REF6 (15) due to sampling inaccuracy of the light table. At the end of Step 1

40 and Step 2, all experiments show evident selective transport or partial mobility, as shown in Figs. S2(c) and S2(d). With the  
 41 increase of flow discharge and sediment supply, the sediment transport regime in all experiments gradually return to equal  
 42 mobility with coarse particles being mobilized at the end of Step 3 and Step 4. The difference of mobility among experiments  
 43 during hydrograph is smaller compared with that at the end of the conditioning phase, and also becomes no longer correlated  
 44 with the duration of conditioning flow.



45  
 46 **Figure S2.** Scaled fractional sediment transport rate at different time of the experiment: (a) start of the conditioning phase ( $t$   
 47 = 15 mins); (b) end of the conditioning phase; (c) end of Step 1 of the hydrograph; (d) end of Step 2 of the hydrograph; (e) end  
 48 of Step 3 of the hydrograph; (f) end of Step 4 of the hydrograph.

49 **References**

- 50 Haynes, H., and Pender, G.: Stress history effects on graded bed stability, *Journal of Hydraulic Engineering*, 33, 343–349,  
51 2007.
- 52 Masteller, C. C., and Finnegan, N. J.: Interplay between grain protrusion and sediment entrainment in an experimental flume,  
53 *Journal of Geophysical Research-Earth Surface*, 122, 274–289, <https://doi.org/10.1002/2017GL076747>, 2017.
- 54 Ockelford, A., Woodcock, S., and Haynes, H.: The impart of inter-flood duration on non-cohesive sediment bed stability, *Earth*  
55 *Surface Processes and Landforms*, 44, 2861-2871, doi:10.1002/esp.4713, 2019.